

THE MELTING BEHAVIOUR OF ALUMINIUM SMELTER CRUST

Qinsong Zhang^{1,2}, Mark P. Taylor¹, John J.J. Chen¹

¹Light Metals Research Centre, and Department of Chemical and Materials Engineering, The University of Auckland, Private Bag 92019, Auckland, New Zealand

²Shenyang Aluminium & Magnesium Engineering & Research Institute Co. Ltd, Shenyang, Liaoning, 110001. P.R. China

Keywords: Crust, Cryolite, Chiolite, Alumina, DTA, Aluminium Reduction cell

Abstract

Crust is the bottom consolidated part of the anode cover, which plays an important role in the performance of aluminium reduction cells. The melting of the crust contributes to the deterioration of the anode cover. Several crust samples were taken from an aluminium smelter. A DTA system was established, and calibrated by measuring the melting temperature of cryolite. The DTA test results show that the melting temperature of the crust samples is depressed due to low cryolite ratio (CR) and high fluoride additives content. In chiolite enriched crust, incongruently melting of chiolite component at 725 °C was detected. Because of the melting of cryolite in the liquid, the chiolite enriched crust had a broader melting temperature range than that with high CR. To our knowledge, few studies have discussed the melting temperature range of the crust and its impact on crust thermal stability at cell operating temperatures.

Introduction

In an aluminium reduction cell, a suitable anode cover should possess sufficient structural strength to support itself above the molten electrolyte. The collapse of the anode cover is mainly caused by two factors, thinning and weakening of the crust and mechanical disturbance. These factors often take effect together. The thinner the crust is the more likely it is to collapse under mechanical disturbance.

Liu et al. [1] measured crust temperature in industrial reduction cell. The melting of the crust bottom is an important cause for the thinning and weakening of it. Liu et al. [1] also measured the liquidus temperature of industrial crust by DSC analysis.

The purpose of this paper was to study the melting behaviour of some industrial crusts from an aluminium smelter in China by differential thermal analysis (DTA) method. It must be noted that the laboratory DTA tests may not correspond exactly with the temperature evolution of the crust in a practical reduction cell.

Experimental

DTA system setup

DTA is widely used for studying the thermal properties of materials. Commercial DTA apparatus is expensive, and fragile to analyze crust samples due to their corrosive liquid and vapour. In this study, a multi sample DTA system was established. The sketch of this DTA system is shown in Figure 1. Laboratory grade α -alumina powder was used as the reference material. For the α -alumina powder, the mean particle size is about 100 μm , and the bulk density is 1.02 g/cm^3 . Four samples and one reference were added into the five graphite crucibles (inner diameter $\text{\O}20\text{mm}$). These crucibles were put in a heating furnace. Figure 1 b shows

the layout of the crucibles with α -alumina as the reference placed in the centre crucible, and samples placed in the four surrounding ones. The DTA tests were conducted under N_2 atmosphere.

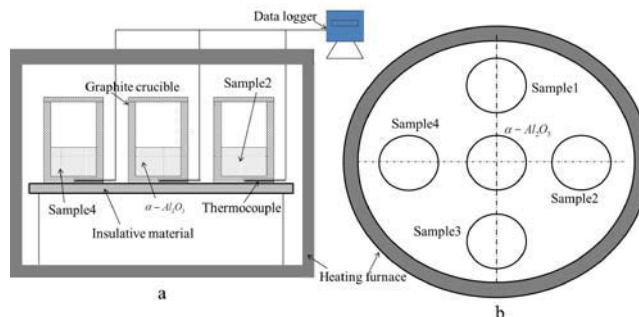


Figure 1. Sketch of the DTA system and sample arrangement

A type N class-2 wire thermocouple was inserted into a hole at the bottom of each crucible (see Figure 2). The distance between the thermocouple and the inner bottom surface of the crucible is about 3mm. The thermocouple was directly connected to a Picologger TC-08 data logger which was connected to a computer. The thermocouple has a tolerance of ± 2.5 °C or $\pm 0.0075 \times T$ between 333 °C and 1200 °C. The data logger has a resolution of 0.01 °C, and was calibrated by a thermocouple calibrator. The samples and the reference were heated to above 1020 °C at a heating rate 1 °C/min. The temperatures of the samples and the reference were recorded by the data logger. Phase transformation in the sample, either exothermic or endothermic, can be detected relative to the reference.

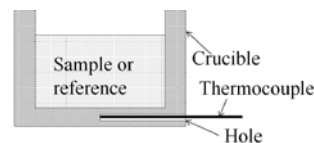


Figure 2. The position of thermocouple in the crucible

Calibration of the DTA system

Compared with commercial DTA systems, the crucible size is larger, and the distance between crucibles is greater in the DTA system for this study. It is normal that the samples and the reference might not be under the exactly same heating condition. Furthermore, the thermocouple may lead to measurement error as well. Thus, it is necessary to calibrate the DTA system.

1) α -alumina powder sample

A DTA test was run with 5g α -alumina powder in the centre crucible as well as in the surrounding crucibles. Figure 3 shows the raw temperature difference curve of the DTA test (sample

temperature minus reference temperature, referred to as raw DTA curve below). The DTA test in this study just recorded the curve above 400 °C where most phase transformations in the crust occur.

Because of the uneven heating condition in the furnace, sample 2 was heated fastest, and had about 4 °C increase in temperature difference between 400 and 700 °C. Therefore, the maximum difference of heating rate between the sample and the reference was estimated as $4/(700-400) \times 1^\circ\text{C}/\text{min}$, which was within $0.015^\circ\text{C}/\text{min}$. The temperature difference kept relatively stable above 700 °C, which indicated that all the samples and the reference had nearly the same heating rate. It is known that the pure α -alumina is inert at the test temperature. As expected, there was no peak detected when the α -alumina sample used. When other sample is used in the DTA test, any peak detected must relate to the phase transformation or reaction in the sample.

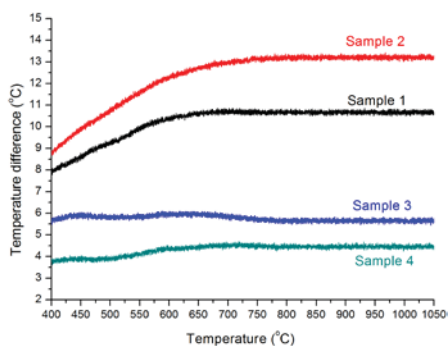


Figure 3. Temperature difference curves of α -alumina samples

The raw DTA curve of α -alumina sample has slight random noise (see Figure 4). The standard deviation (SD) of the noise is less than 0.07. In addition, the temperature difference varies within a range of 0.2 °C. In order to eliminate the noise, the DTA curve was smoothed by Savitsky-Golay smoothing method (referred to as smoothed DTA curve below). In Figure 4, the two nearly straight lines are the temperature curves of the sample and the reference.

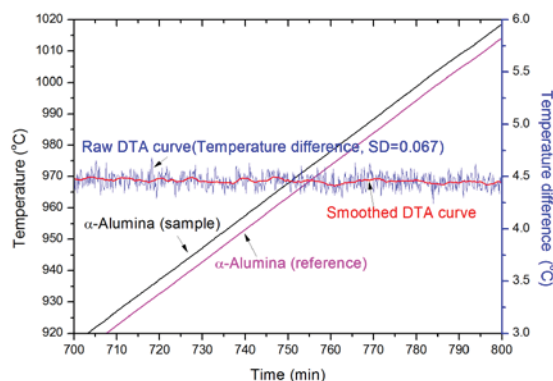


Figure 4. Example of the random noise of the DTA curve

2) Cryolite powder sample

Laboratory grade cryolite powder samples were used to calibrate the DTA system. For the cryolite powder, the mean particle size is about 80 μm , and the bulk density is $1.31\text{ g}/\text{cm}^3$. Its CR is 2.94. The weights of the cryolite powder samples in four crucibles are 2 g, 3 g, 3 g and 5 g respectively.

The $\alpha \leftrightarrow \gamma$ and crystal \leftrightarrow liquid phase transformations of pure cryolite have been widely studied and included in the NIST-JANAF thermochemical tables [2]. The $\gamma \leftrightarrow \delta$ phase transformation of cryolite at 881 °C was detected by Landon [3]. Table 1 shows the temperature and enthalpy of these phase transformations.

Table 1. Phase transformations of cryolite [2,3]

Phase transformation	Temperature °C	Enthalpy (kJ/kg)
$\alpha \leftrightarrow \gamma$	565	45
$\gamma \leftrightarrow \delta$	881	<4
crystal \leftrightarrow liquid	1011	524

Figure 5 shows the smoothed DTA curves of cryolite samples with identified phase transformations. All $\alpha \leftrightarrow \gamma$ and crystal \leftrightarrow liquid phase transformations are identified. No $\gamma \leftrightarrow \delta$ phase transformation is identified possibly due to its very low enthalpy.

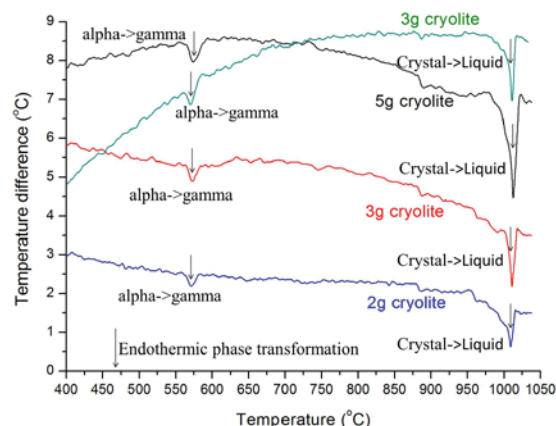


Figure 5. Phase transformation identification from DTA curves (peak is indicated by arrow) (two 3g cryolite samples are located differently)

In general, the melting point is defined as the extrapolated onset temperature (T_e), which is the temperature at the intersection of the extrapolated baseline prior to the peak with the extrapolated rising edge of the peak [4]. In many cases, it is difficult to determine the extrapolated onset temperature very accurately. The melting peak temperature (T_p), which is the clearest characteristic temperature, is also used as melting point [5].

The measured melting temperature of the cryolite is summarized in Table 2. The cryolite is extremely close to the pure compound - the theoretical melting temperature of it is likely to be between 1010 and 1011 °C according to Haupin's measurement [6]. Thus, the maximum measurement error of the DTA system is about 4 °C. The error might be caused by the temperature gradient in the sample and the crucible, and/or the thermocouple tolerance.

Table 2. Measured melting temperature of the cryolite

Weight (g)	T_e (°C)	T_p (°C)	Peak height (°C)
2	1006.8	1009.7	1.3
3	1006.8	1010.8	2.0
3	1006.8	1010.8	2.0
5	1006.8	1013.2	2.9

There were two 3g cryolite samples in crucibles located differently in the DTA system. Though the DTA curves are not exactly the same, they give the same measured melting temperature result. The influence of the location of the crucible on the measurement result is thus negligible. For samples of 2 to 5 g, the peak height is clear enough for phase transformation identification. At the same time the measurement error is acceptable as shown by the discussion above. Hence, it is reasonable to conclude that the DTA system was calibrated by measuring the melting temperature of the cryolite.

Industrial crust samples

Seven crust pieces were taken from a couple of industrial reduction cells. Figure 6 shows the positions from which they were taken. They are referred to as Crust A, B, C, D, E, F, and G.

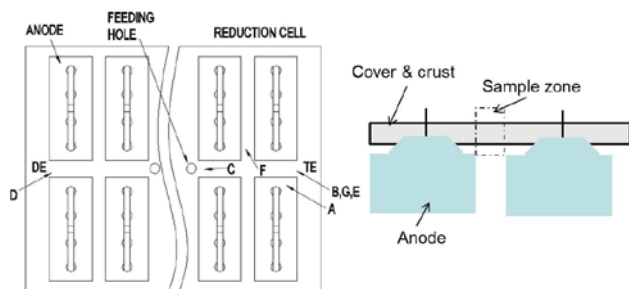


Figure 6. The positions from which industrial crust pieces were taken.

Several samples were taken from different vertical positions of these crust pieces. Each sample was crushed by a hammer mill into a fine powder and dried (~8 hours, 150 °C).

The chemical compositions of these samples were analyzed by XRD phase analysis and Rietveld refinement. To determine alumina content, the oxygen contents of some samples were measured by using a LECO RO-416DR Oxygen Determinator fitted with a model EF-400 Electrode Furnace (LECO Corporation, St. Joseph, MI).

Phase transformations of these crust samples at 400~1020°C were analyzed by the DTA test. In each DTA test, four different crust samples were put in the four sample crucibles respectively. The weight of each crust sample is 5g.

Cryolite/alumina powder mixture samples

Cryolite and alumina are the major composition of the industrial crust. The binary system cryolite-alumina has been well studied [7]. In this study, the cryolite and α -alumina powder were mixed together evenly as 5g samples with various α -alumina content (5%, 35%, 45%) respectively. Thermal analysis of the mixture samples was carried out by the DTA test. The results of them and the cryolite were used to verify the single phase transformation peak shape, against the multi-phase peak shape results of the later crust samples.

Results and discussions

Smoothed DTA curves

The smoothed DTA curves of the cryolite/alumina mixture samples and eight representative crust samples are shown in Figure 7 and Figure 8 respectively. Peaks below 600 °C seem to be α - γ cryolite phase transformation which are not within the scope of this study. In the temperature range 600~1020 °C, one or two distinct peaks at the DTA curve of each sample were detected. The melting peak temperature was determined. However, it is noted that alumina enriched sample may not completely melt into liquid phase above the melting peak temperature.

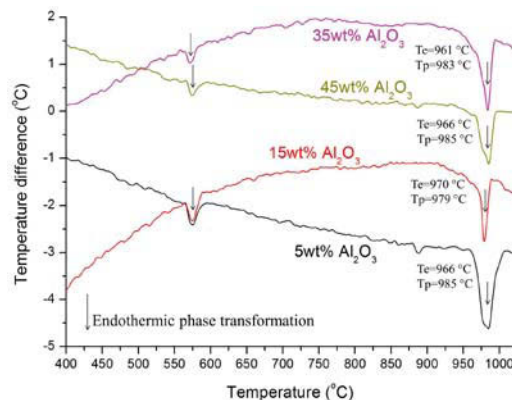


Figure 7. DTA curve of 5g cryolite/alumina mixture

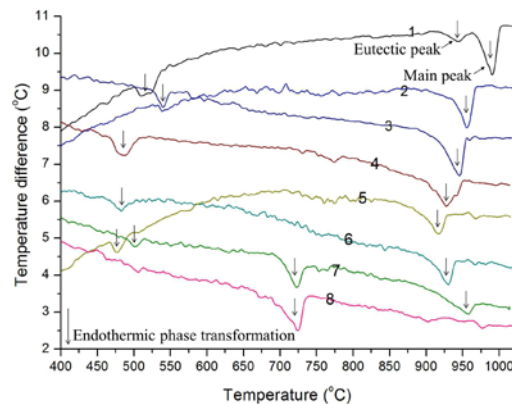


Figure 8. DTA curves of crust samples (the melting temperature of each sample is given in Table 3)

Melting temperature depression

1) Cryolite/alumina mixture

The cryolite/alumina mixture is considered to be a simple eutectic system [7,8]. As reported in the literature, the eutectic alumina concentration is 10.0-11.5 wt%, and the eutectic temperature is 960-966 °C [7,8]. This eutectic temperature is also the liquidus temperature measured from cooling process if a dissolved alumina concentration approaching the eutectic is achieved. According to the heating DTA curve in this study, the melting extrapolated onset temperatures of the cryolite/alumina mixture are 961-970 °C.

2) Industrial crust

The major chemical composition and melting temperature of these eight crust samples are listed in Table 3. Detailed results of all the crust samples refers to the previous paper in this series [9]. These crust samples contain cryolite, chiolite, alumina and other

additives including AlF_3 , K_2NaAlF_6 , $\text{LiNa}_2\text{AlF}_6$, CaF_2 , $\text{Na}_2\text{LiAlF}_6$ et al.

Table 3. Major chemical composition and melting temperature of some crust samples

Sample No.	Description	Major composition wt%			CR	Te (°C)	Tp (°C)
		Alumina	Cryolite	Chiolite			
1	Macrocrystalline crust	0.49	73.1	4.1	2.64	971	990
2	Crust A (1cm)	25.83	50.8	6.7	2.53	936	956
3	Crust B (2cm)	2.3	61.7	4.8	2.54	914	945
4	Microcrystalline crust	2.93	49.7	5.4	2.42	906	927
5	Crust D (3cm)	27.49	39.8	3.0	2.35	893	917
6	Crust C (2cm)	31.60	32.4	7.2	2.28	909	930
7	Crust G bottom	1.5	34.4	41.6	2.06	700*	725*
8	Crust G top	1.69	4.7	80.1	1.74	704*	725*

Note: *: incongruent melting of chiolite; (1cm): distance to the bottom surface of sintered crust, composition data with underline is from LECO Oxygen Analysis, data without underline is from semi-quantitative XRD Rietveld refinement. Some data is updated and may slightly differ from previous paper.

The melting temperature of the crust samples decreases with the decrease of CR in general, as shown in Figure 6. The extrapolated onset temperature of crust samples 4~7 was depressed to about 900 °C.

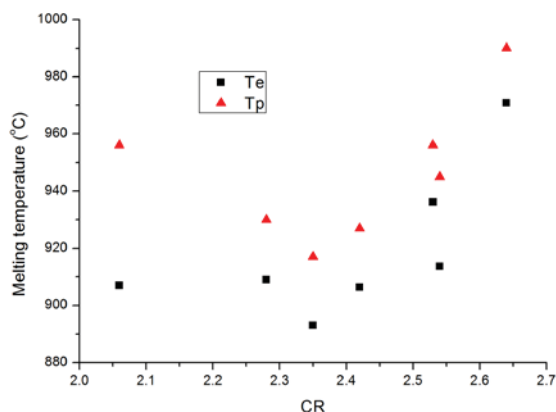
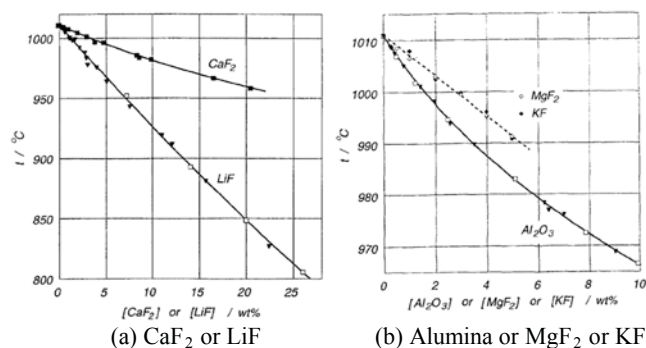


Figure 9. The influence of CR on melting temperature

It has been studied that alumina and fluoride additives depress the liquidus temperature of molten cryolite greatly, as shown in Figure 10. It is very likely that they also depress the melting temperature of the crust. Like the cryolite/alumina mixture, the crust samples may be a eutectic mixture consisting of cryolite, alumina and additives.



(a) CaF_2 or LiF

(b) Alumina or MgF_2 or KF

Figure 10. Liquidus temperature of cryolite with addition of alumina, CaF_2 , MgF_2 , LiF and KF [10].

In the case of crust sample 1, a very small peak is detected before the main peak (see Figure 8). However it does not affect the determination of melting temperature. In fact, this DTA curve seems a typical curve of eutectic mixture [11,12]. The extrapolated onset temperature (921 °C) of this small peak, called eutectic peak, is the eutectic temperature of the crust sample. Eutectic peak may be integrated with the main peak or fail to be detected for some crust samples in this study.

The incongruent melting of chiolite ($\text{Na}_5\text{Al}_3\text{F}_{14}(\text{s}) + \text{Al}_2\text{O}_3(\text{s}) = \text{Na}_3\text{AlF}_6(\text{s}) + \text{Liquid}$) around 725 °C was detected from crust samples 7 and 8 which have high chiolite content. No such peak was detected from other crust samples due to the low chiolite content.

Melting behaviour study by peak shape analysis

Peak shape is an important feature of DTA curve for qualitative study. It has been used to study phase diagram [13] and reaction kinetics [14,15].

For a DTA system, the peak shape relates to the heating rate, and sample properties such as thermal conductivity, granular size, etc [16]. Figure 11 shows the peak shapes of the cryolite and cryolite/alumina mixture samples. The sample weight seems to have little impact on the peak shape. All cryolite samples have similar sharp peak when the weight of them decreases from 5g to 2g in spite of the decreasing of the peak height.

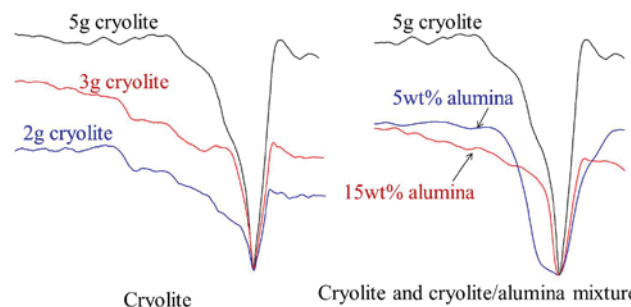


Figure 11. Peak shapes of the cryolite and cryolite/alumina mixture samples

(1) Hypothesis and verification

Compared with the nearly pure cryolite, the 5wt% alumina mixture has a much broader peak in Figure 12. However, the peak becomes narrower when alumina content increases to 15wt%. Though the slight difference of the physical properties between the samples may contribute to the peak shape difference, the melting behavior is very likely the dominant cause, as explained below.

Our hypothesis is that the sample is heated/cooled slowly enough to reach phase equilibrium during the DTA test. Thus the melting behaviour follows the phase diagram as shown in Figure 12. Solheim et al. [7,10] have proposed empirical expressions for the two line EA and EB in the phase diagram.

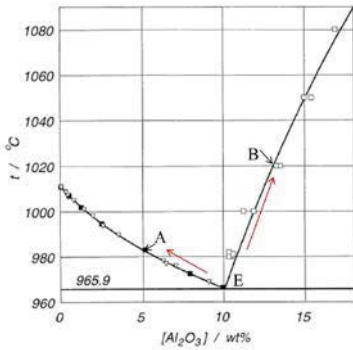


Figure 12. The liquidus diagram for the binary system Na_3AlF_6 - Al_2O_3 [7] (E is the eutectic point).

The way that fusion enthalpy is absorbed during the phase transformation may be the reason for the difference peak shapes between the cryolite, 5 wt% and 15 wt% alumina mixtures. When pure cryolite melts, all fusion enthalpy is absorbed at an almost fixed temperature, and a very sharp peak forms. In the case of the 5 wt% alumina mixture, 5wt% alumina + 45wt% cryolite melts at eutectic temperature, and the remaining 50wt% cryolite melts into the liquid between the eutectic temperature and 985 °C, which is explained by the line EA in the phase diagram (see Figure 12). The melting rate is calculated to be 2.63wt%cryolite/°C. For the 15 wt% alumina mixture, 9.44wt% alumina + 85wt% cryolite melts at the eutectic temperature, and then the composition of the liquid moves along the line EB in the phase diagram (see Figure 12). The dissolving rate is about 0.053wt%alumina/°C.

The fusion enthalpy of cryolite is 524 kJ/kg [2]. According to Phan-Xuan's measurement [17], the partial enthalpy of the dissolution of alumina in liquid bath was 1431 kJ/kg when the alumina concentration was more than 6 wt%. The corresponding endothermic enthalpy changes (equal to melting/dissolving rate times enthalpy) along line EA (5wt% alumina mixture) and EB (15wt% alumina mixture) are 1378 kJ/(kg°C) and 76 kJ/(kg°C) respectively.

The melting behaviour of 15wt% alumina mixture follows closely that of pure cryolite, and most fusion enthalpy is absorbed at the eutectic temperature. Whereas for the 5wt% alumina mixture, only about half of the fusion enthalpy is absorbed at the eutectic temperature, and other half fusion enthalpy is absorbed between the eutectic temperature and 985 °C. In this case, the eutectic peak is integrated with the main peak to form the broad peak.

(2) Melting behaviour of the crust

Based on the comparison of the melting behaviours of the well studied materials such as pure cryolite and cryolite/alumina mixture, the peak shape relates to the melting behaviour.

Figure 13 shows peak shapes of some crust samples. The peak tends to become broader when the CR decreases. For instance, crust samples 6 and 7 have close original cryolite content, but the latter has much higher chiolite content. Because chiolite incongruently melts to solid cryolite and liquid, crust sample 7 contains more solid cryolite and also liquid above 725 °C. According to the phase equilibrium hypothesis, solid cryolite continuously melts in the liquid over a very wide temperature range (from 725 °C to the melting temperature). Other fluoride additives may also dissolve in the liquid. For the crust sample

with low chiolite content, less liquid melts from chiolite, and thus less solid cryolite melts in the liquid. This may explain that the peak shape of crust sample 7 is distinctly broader than that of crust sample 6. The crust sample 1 is dominated by the eutectic mixture of cryolite, alumina and additives, and melts in a relative narrow temperature range.

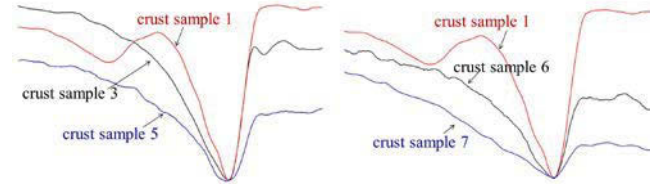


Figure 13. Peak shape of the crust samples

(3) Crust thermal stability

Liu [1] measured the crust temperature in two industrial cells, as shown in Figure 14. The measurement started from the time that the anode cover was added in the cells. The heating rate was below 1.6 °C/min. The measured chiolite content in the bottom 2-3cm of the crust in Cell A and B were 20.4 wt% and 38.7 wt% respectively. The crust in Cell B seemed to have lower temperature but melt faster than that in Cell A (see Figure 14). According to the present study, higher chiolite content results in more liquid above 725 °C, which then melts more cryolite. This probably explains the faster melting of crust in Cell B.

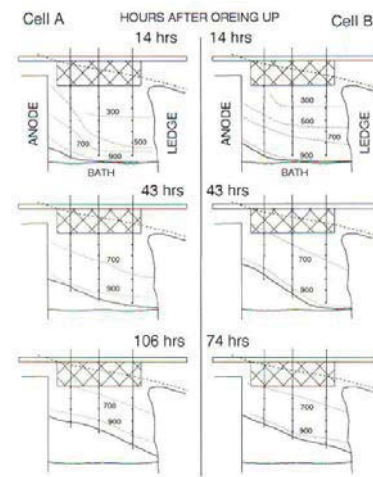


Figure 14. Crust isotherm measured by Liu [1]

In addition, Liu [1] observed that the occurrence of anode effect (AE) in the cell broke the bottom crust. The loss of large amounts of the crust bottom occurred after the AE in Cell A. It is known that a great amount of energy is released quickly during the AE, and a considerable portion of it is likely to be transferred to the crust. The energy in the crust which can not be conducted to the surroundings in time turns into sensible and latent heat. When the absorbed latent heat exceeds the fusion enthalpy of the crust, at least the bottom part of it will melt and collapse.

The analysis in this study shows that the melting of the crust with high CR is energy intensive in a narrow temperature range. Whereas, the chiolite enriched crust melts continuously in a broad temperature range. The crust with lower chiolite content and higher CR has higher hot strength (less liquid) and better thermal

stability. High alumina content in crust would also contribute to good thermal stability but unfortunately high alumina (>20% added to anode cover) also reduces the thermal conductivity of the original anode cover [18] and causes rapid overheating of the material followed by accelerated melting as found by Liu [1]. Reducing anode movements (eg. reduced AE frequency) is another way to avoid the collapse of the crust. However metal tapping will still trigger crust collapse for thermally unstable (melting) material.

Conclusions

A multi sample DTA system was developed to measure the melting temperature of industrial crust. The system has been calibrated by measuring the melting temperature of cryolite. The measurement error is up to 4 °C when the heating rate is as slow as 1 °C/min. The melting temperature of the crust usually ranges from 725 to 1000 °C depending on the additives in it. The measurement error of 4 °C is acceptable for this temperature range. The system has been shown to be useful for the study of the melting behaviour of industrial crust.

The melting temperature of the industrial crust depends on its chemical composition. The crust with higher CR has higher melting temperature and narrower melting temperature range. The melting of solid cryolite into lower melting liquid is a significant factor in the melting of chiolite enriched crust. In order to make the crust durable, it is necessary to avoid high contents of low melting component such as chiolite in the anode cover and to ensure adequate thermal transmission of heat through the anode cover applied originally to the cell.

It should also be noted here that the liquid produced in the crust samples here stay with the solid during the whole DTA test performed, while in industrial smelting cells the liquid is observed to drop down to the bulk liquid bath of the cells before the complete melting of the solid cryolite.

Acknowledgements

The authors appreciate the assistance given by Mr. David Cotton in carrying out the experiments.

References

1. X. Liu et al., "Crust Formation and Deterioration in Industrial Cells," *Light Metals*, (1992), 489-494.
2. M. W. Chase et al., *Nist-Janaf Thermochemical Tables*. (American Chemical Society, 1998),
3. G. Landon and A. Ubbelohde, "Melting and Crystal Structure of Cryolite (3naf, AlF₃)," *Proc. R. Soc. London, Ser. A* **240**(1221)(1957), 160-172.
4. S.-D. Clas et al., "Differential Scanning Calorimetry: Applications in Drug Development," *Pharm. Sci. Technol. Today* **2**(8)(1999), 311-320.
5. B. E. Yoldas, "Thermal Stabilization of an Active Alumina and Effect of Dopants on the Surface Area," *Journal of materials science*, **11**(3)(1976), 465-470.
6. W. Haupin, "The Influence of Additives on Hall-Héroult Bath Properties," *JOM(USA)*, **43**(11)(1991), 28-29.
7. E. Skybakmoen et al., "Alumina Solubility in Molten Salt Systems of Interest for Aluminum Electrolysis and Related Phase Diagram Data," *Metall. Mater. Trans. B* **28**(1)(1997), 81-86.
8. K. Grjotheim and C. Krohn, *Aluminium Electrolysis: Fundamentals of the Hall-Heroult Process*. (International Publishers Service, Incorporated, 1982), 31.
9. Q. Zhang et al., "Composition and Thermal Analysis of Crust Formed from Industrial Anode Cover," *Light Metals*, (2013), 673-680.
10. A. Solheim et al., "Liquidus Temperatures for Primary Crystallization of Cryolite in Molten Salt Systems of Interest for Aluminum Electrolysis," *Metall. Mater. Trans. B* **27**(5)(1996), 739-744.
11. W. L. Chiou, "Mechanism of Increased Rates of Dissolution and Oral Absorption of Chloramphenicol from Chloramphenicol - Urea Solid Dispersion System," *Journal of pharmaceutical sciences*, **60**(9)(1971), 1406-1408.
12. M. Matsuoka and R. Ozawa, "Determination of Solid-Liquid Phase Equilibria of Binary Organic Systems by Differential Scanning Calorimetry," *Journal of Crystal Growth*, **96**(3)(1989), 596-604.
13. S.-W. Chen et al., "The Relationship between the Peak Shape of a DTA Curve and the Shape of a Phase Diagram," *Chemical engineering science*, **50**(3)(1995), 417-431.
14. H. E. Kissinger, "Reaction Kinetics in Differential Thermal Analysis," *Analytical chemistry*, **29**(11)(1957), 1702-1706.
15. R. L. Reed et al., "Differential Thermal Analysis and Reaction Kinetics," *Industrial & Engineering Chemistry Fundamentals*, **4**(1)(1965), 38-46.
16. R. Melling et al., "Study of Thermal Effects Observed by Differential Thermal Analysis. Theory and Its Application to Influence of Sample Parameters on a Typical DTA Curve," *Analytical chemistry*, **41**(10)(1969), 1275-1286.
17. D. Phan-Xuan et al., "Microcalorimetric Study of Alumina Dissolution in Cryolite Baths," *Light Metals*, (1975), 159-178.
18. M. P. Taylor, "Anode Cover Material - Science, Practice and Future Needs," *Proceedings of 9th Australasian Aluminium Smelting Technology Conference*, (2007).